Luminescence of double quantum wells subject to in-plane magnetic fields

M. Orlita,* R. Grill, P. Hlídek, and M. Zvára
Faculty of Mathematics and Physics, Charles University, Institute of Physics, Ke Karlovu 5, CZ-121 16 Prague 2, Czech Republic

G. H. Döhler and S. Malzer
Max-Planck-Research Group, Institute of Optics, Information and Photonics, Universität Erlangen-Nürnberg, D-91058 Erlangen, Germany

M. Byszewski
Grenoble High Magnetic Field Laboratory, Boîte Postale 166, F-38042 Grenoble Cedex 09, France
(Received 13 April 2005; revised manuscript received 19 August 2005; published 11 October 2005)

We report on photoluminescence (PL) measurements of a symmetric GaAs/AlGaAs double quantum well (DQW) in high magnetic fields. For this study, a selectively contacted p-δn–DQW–δn-p structure was chosen, allowing an independent tuning of the electron density in the DQW and thus a creation of a two-dimensional electron gas. Our attention was focused on phenomena in in-plane magnetic fields, where the field-induced depopulation of the antibonding subband observable in the PL spectra as a so-called N-type kink was predicted by Huang and Lyo (HL) [Phys. Rev. B **59**, 7600 (1999)]. Whereas the equivalent behavior has been observed several times in the electric transport measurements and a proper theoretical description has been found, to the best of our knowledge, no PL experiment in a direct comparison with the theoretical model developed by HL has ever been published. We carried out a self-consistent calculation based on their model and achieved a good agreement with our experimental results. Additionally, the influence of the excitonic interaction on the PL spectra, not taken into account by HL, is also discussed. This enables us to explain small deviations from the HL theory. The interpretation of the in-plane magnetic field measurements is supported by the experiment with the magnetic field in the perpendicular orientation that allows a sufficiently accurate estimation of the electron density in the DQW. Distinctive renormalization effects of DQW subbands at various electron densities are also observed and discussed.

DOI: 10.1103/PhysRevB.72.165314 PACS number(s): 78.67.De, 78.55.Cr, 73.21.Fg, 78.20.Ls

I. INTRODUCTION

Double quantum wells (DQW) have been attracting a great deal of attention owing to their challenging properties, particularly formation of spatially direct and indirect excitons and their possible condensation to a cold exciton gas at low temperatures.[1,2] While in the configuration with the magnetic field perpendicular to the quantum well (QW) plane a free in-plane motion of charge carriers is quantized into Landau levels, an in-plane magnetic field (parallel to the layers) changes the carrier energy dispersion in the QW plane in the direction perpendicular to the field. Since Lyo's theoretical prediction of a saddle point type van Hove singularity in the density of states of a DQW, induced by an in-plane magnetic field,[3] much effort has been devoted to confirm this prediction experimentally. Another simple bi-layer quantum structure, similar to DQW, can be created in a rather broad modulation-doped single quantum well by a sufficiently high parallel magnetic field.[4,5] The predicted singularity in the magnetic-field-dependent density of states was at first successfully confirmed on both types of bi-layer systems in electric transport measurements—a modulation of the in-plane electric conductance[6–8] and of the cyclotron mass[9] in the in-plane magnetic field was reported. Among latest results concerning these effects, we mention thermopower measurements on the DQW system performed by Fletscher *et al.*[10] They have measured a clear dependence of the thermopower on the applied in-plane magnetic field and supported the experimental results by a convincing theoretical description.

It has become a challenge to find a manifestation of phenomena predicted for the in-plane magnetic field also in optical experiments. The photoluminescence (PL) calculation of DQW in the in-plane magnetic field, neglecting excitonic interaction between electron and hole, was published by Huang and Lyo.[11] The PL investigation of a similar bi-layer system in the in-plane magnetic field was reported by Whittaker *et al.*,[12] where the one-side modulation doping of a wide QW ensured a large separation of electrons and holes due to the strong built-in electric field. The observed strong quadratic shift of the luminescence maximum with in-plane magnetic field was interpreted as a result of the field-induced indirect gap. Similar measurements on wide QWs and heterojunctions have very recently been carried out by Ashkinadze *et al.*[13] Other in-plane magneto-optical measurements, in this case already on symmetric DQW structures, were published by Kim and co-workers.[14,15] In a parallel field, they observed two resolved peaks and their shift to the higher energy with increasing magnetic field. The peaks were related to the recombination of electrons from an upper (antibonding) subband-created by an antisymmetric linear combination of wave functions of a single QW, and from a lower (bonding) subband formed by a symmetric combination of electron states of a single well. In accordance with theoretical predictions,[11] they observed a $\mathcal{N}$-type kink, i.e., a gradual depopulation of the electron and hole antibonding subband resulting in a redshift of the PL maximum followed by its

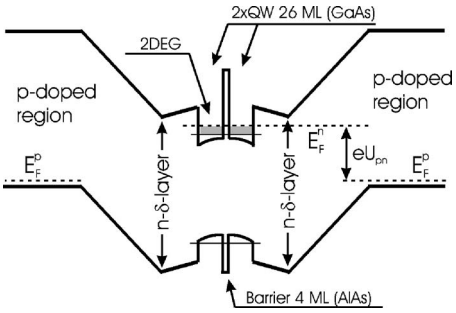

FIG. 1. The schematic picture of the studied sample under a typical operational condition $U_{pn}>0$. E_F^p and E_F^n denote Fermi level in *p*-doped regions and 2DEG, respectively. Lengths are not in scale.

blueshift, reflecting a diamagnetic increase of the bonding subband energy. However, no comparison with theoretically calculated spectra was performed.

In this paper, we present a study of PL from a symmetric DQW with various electron density in the magnetic field in perpendicular (Faraday), as well as in parallel (Voigt), orientation. The paper is organized as follows. In Sec. II a brief description of experiment and the studied sample is provided. The simple theory of phenomena in the in-plane magnetic field is summarized in Sec. III. Section IV concerns us with experimental results. These are compared with the suggested theory and the applicability of the used theoretical model is discussed with respect to the excitonic interaction, whose effects dominate the PL spectra at low carrier densities. Finally, the conclusions are given in Sec. V.

II. EXPERIMENT

Our magnetoluminescence measurements were carried out on a *p-i-δn*–DQW–*δn-i-p* structure grown by molecular beam epitaxy (MBE). A simple scheme of this structure under a typical operational condition is shown in Fig. 1. The symmetric DQW consists of two 26 ML, i.e., ≈7.5-nm-thick GaAs QWs with a 4 ML AlAs barrier in between. This DQW is separated from *δ-n*-doped layers by 30-nm-thick $Ga_{0.7}Al_{0.3}As$ spacers. Both GaAs/$Ga_{0.7}Al_{0.3}As$ interfaces in the DQW are smoothed by a 1 ML AlAs layer. The *δ-n* doping is realized by a 1-nm-thick *n*-doped $Ga_{0.7}Al_{0.3}As$ (Si, 1.5×10^{18} cm^{-3}) layer, which corresponds to the 2D donor density $n_D^{(2)}=1.5\times10^{11}$ cm^{-2}. The thickness of the $Ga_{0.7}Al_{0.3}As$ intrinsic part located between the *δ-n* layer and *p*-doped region is 350 nm on both sides. A doping density (C, 2.0×10^{18} cm^{-3}) is used in both *p*-doped regions. The sample was photolithographically processed, i.e., the structure was mesa etched, isolated and selectively contacted to the *p*-doped regions and to the region involving the DQW and the *δ-n* layers. The design of the sample was chosen to allow for a tuning of the electron density by applying a *p-n* bias with both *p* contacts kept at the same potential. When no bias is applied to the sample in the dark, the relatively weakly doped *δ-n* layers supply a negligible electron density in the DQW. As schematically depicted in Fig. 1, a two-dimensional electron gas (2DEG) with a tunable density is created at a positive bias U_{pn}. In the flat-band regime, when no electric field is present in intrinsic regions, the 2DEG density close to the *δ-n* doping ($\approx3\times10^{11}$ cm^{-2}) is achieved. The influence of the optical excitation on the electron density will be discussed later on. The PL spectra presented in this paper were gained from several mesa structures taken from the same wafer. All investigated structures exhibited almost identical behavior showing thus a very good homogeneity of MBE growth.

The sample was excited by a Ti:sapphire laser with a standard power density $I_0\approx100$ mW/cm^2 at the photon energy 1.72 eV, i.e., below the band gap of $Ga_{0.7}Al_{0.3}As$ at a helium temperature. An optical fiber was used for the excitation, as well as for the signal collection. The PL spectra were analyzed by a monochromator and detected by a cooled charge coupled camera. The helium bath cryostat ensured a good sample temperature stability at 4.2 K. All measurements were performed in a resistive solenoid up to the magnetic field of 22 T in the Voigt or Faraday configuration.

III. THEORY

The theoretical description discussed below follows a simplified model suggested by Huang and Lyo,[11] where no excitonic effects are included. In zero magnetic field, the electron subband energies E_e^i and corresponding wave functions $\chi_i(z)$ can be obtained straightforwardly using a common self-consistent procedure. This involves a simultaneous solution of the one-dimensional (1D) Schrödiner equation written in the envelope function approximation (EFA):

$$\left(-\frac{\hbar^2}{2m_e}\frac{d^2}{dz^2}+V_e(z)\right)\chi_e^i(z)=E_e^i\chi_e^i(z), \tag{1}$$

and the Poisson equation:

$$\frac{d^2}{dz^2}V_H(z)=-\frac{e^2n^{(2)}}{\epsilon_0\epsilon_r}\sum_i|\chi_e^i(z)|^2, \tag{2}$$

where $V_H(z)$ is the Hartree potential, which appears also in the potential energy $V_e(z)$:

$$V_e(z)=V_H(z)+E_c(z)+V_{xc}(z), \tag{3}$$

together with $E_c(z)$ and $V_{xc}(z)$ denoting the DQW conduction band profile and the exchange-correlation potential, respectively. In accordance with HL,[11] the approximation for $V_{xc}(z)$ was taken from Hedin and Lundqvist.[16] Overall in the paper, the lowest lying bonding $i=1$ and antibonding $i=2$ subbands are taken into account only. ϵ_0 and ϵ_r denote vacuum and relative permittivity, respectively. Because the 2D electron density $n^{(2)}$ serves as an input parameter of our calculation and the symmetric DQW only is considered, we can use the boundary condition:

$$\lim_{z\to-\infty}\frac{dV_H}{dz}=-\lim_{z\to+\infty}\frac{dV_H}{dz}=\frac{e^2n^{(2)}}{2\epsilon_0\epsilon_r}. \tag{4}$$

All z-dependent material parameters such as the relative permittivity ϵ_r or the relative mass of electron and hole m_e, m_h, are taken as an averaged value in our calculation.

Henceforth we take the in-plane magnetic field $\mathbf{B}=(0,B_\parallel,0)$ with the vector potential gauge $\mathbf{A}=(B_\parallel z,0,0)$ into account. The field modifies the Schrödinger equation (1), where an additional $B_\parallel$-dependent term parabolic in z appears:[11]

$$\left[-\frac{\hbar^2}{2m_e}\frac{d^2}{dz^2}+\frac{\hbar^2}{2m_e}\left(k_x-\frac{eB_\parallel z}{\hbar}\right)^2+V_e(z)\right]\chi^i_{e,k_x}(z) = E^i_e(k_x)\chi^i_{e,k_x}(z). \quad (5)$$

In the in-plane magnetic field, the electron in-plane motion becomes coupled with the motion in the z direction and thus the electron wave function χ^i_{e,k_x} and subband energy $E^i_e(k_x)$, are implicitly dependent on the electron momentum in the x direction k_x. The motion in the y direction, i.e., along the applied magnetic field $B_\parallel$, remains uncoupled and therefore the whole electron energy in the ith subband can be written in the form

$$\mathcal{E}^i_e(k_x,k_y)=E^i_e(k_x)+\frac{\hbar^2k_y^2}{2m_e}. \quad (6)$$

In general, Eq. (5) requires again a self-consistent solution to find $V_e(z)$. However, we suppose that the magnetic-field-induced changes in the potential $V_e(z)$ are small in comparison with a strong additional z-dependent parabolic term in Eq. (5). Therefore, we use the potential $V_e(z)$ achieved at zero magnetic field and avoid thus a complicated calculation. This assumption cannot be successfully used for asymmetric DQWs, where magnetic field $B_\parallel$ induces a significant redistribution of the total charge between wells, which strongly affects the Hartree term $V_H(z)$ contained in the total potential $V_e(z)$.

Up to now, we dealt with electron states only. To calculate hole states in the DQW, we solve again Eq. (1) or optionally in the nonzero magnetic field Eq. (5). In this case, we have to take an appropriate hole mass m_h and replace the total electron potential $V_e(z)$ by the total potential for holes $V_h(z)$, which includes the valence band profile $E_v(z)$ and the Hartree term $-V_H(z)$. In accord with our experiment, the density of the photogenerated holes is supposed to be much less than $n^{(2)}$. Hence, the Hartree term is given by the spatial distribution of electrons only and the exchange-correlation effects in the hole gas are neglected. Note that we consider the heavy hole states only in agreement with HL.[11] No nonparabolic or valence band mixing effects are included.

The luminescence intensity $I(\omega)$ roughly corresponds to the local joint density of states modified by the Fermi-Dirac statistical distribution of electrons and holes $f_e(E)$, $f_h(E)$:

$$I(\omega)\propto\sum_{k_x,k_y,i,j} f_e(E^i_e),f_h(E^j_h)|\langle\chi^j_h|\chi^i_e\rangle|^2\,\delta(E^i_e-E^j_h-\hbar\omega). \quad (7)$$

Optical transitions between bonding and antibonding subbands ($j\neq i$) must be included, because this recombination becomes allowed at a finite in-plane magnetic field.

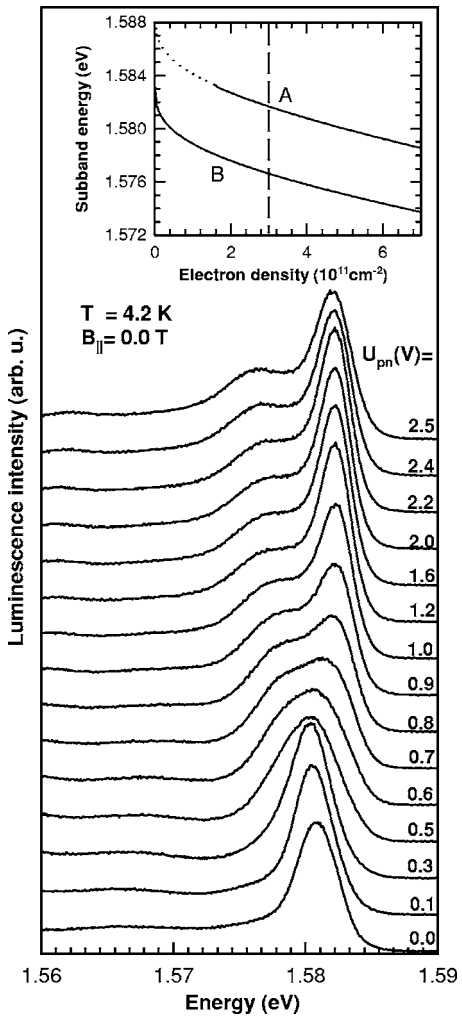

FIG. 2. PL spectra at zero magnetic field for various applied positive bias U_{pn}. The p contacts were kept at the same potential. The inset contains recombination energy calculated for electrons in the bottoms of the B and A subbands as a function of the electron density in DQW. The dotted line shows the unoccupied antibonding subband at lower electron densities. The dashed line denotes the total intended doping of δ-n layers.

IV. RESULTS AND DISCUSSION

A. PL as a function of applied bias

We start the discussion with the analysis of results in Fig. 2, which shows PL spectra of the studied sample at zero magnetic field as a function of the applied bias U_{pn}. Both p contacts were kept at the same potential, as well as in all other measurements presented in this paper. The observed spectrum consists of a well pronounced PL structure in the spectral range 1.575–1.585 eV and of a significant low-energy tail that will be commented on later. The sample was designed to obtain a depleted DQW at $U_{pn}=0.0$ V and a 2DEG density corresponding to the total charge of δ-n doping ($2n_D^{(2)}=3\times10^{11}$ cm^{-2}) in the flat-band regime. The flat-band regime is achieved for $U_{pn}\cong+1.8$ V at liquid helium temperature. Taking account of this, the relatively narrow PL line at $U_{pn}=+0.0-0.3$ V can be assigned to the excitoniclike

recombination and the line broadening observed above $U_{pn} = +0.5$ V reflects the formation of 2DEG and further increase of its density at higher bias. Simultaneously, the low-energy edge of the PL line shifts towards lower energies due to the subband renormalization, confirming the gradual increase of the electron density. At $U_{pn} \approx +1.2$ V, a steplike shape of the PL spectrum is achieved and this shape remains practically unchanged up to the bias of $U_{pn} \approx +2.0$ V, then a further redshift of the low-energy edge appears, showing thus a further increase of the electron density. The interpretation of the PL spectra at U_{pn} above the flat-band regime is not straightforward. In this case, the total applied bias U_{pn} can drop not only on the *p-n* junction, being in the forward regime, but also in the *p*- and *n*-contact layers themselves. However, an approximately exponential course of the current through the *p-n* junction with U_{pn} suggests that the voltage lost in the contacts is not dominant in the chosen interval of bias voltage ($U_{pn} < 2.6$ V).

The shape of the spectrum can be interpreted on the basis of the self-consistent calculation depicted in the inset of Fig. 2, where the recombination energies for electrons in the bottom of the bonding (B) and antibonding (A) subbands are shown as a function of the 2D electron density. Hence, these values represent the energies of steps in the joint density of states, or in corresponding points of inflection in the PL spectra, when the realistic broadening of the PL spectra is taken into account. The difference in transition energies is given by the splitting of electron subbands B and A only, holes are supposed to be localized, having their energy at the bottom of the hole subband B, as is elucidated later on. The presented calculation predicts a relatively steep decline of the recombination energy at very low densities $n_e < 10^{11}$ cm^{-2}. However, this expectation is unrealistic due to the excitonic effects completely neglected in the calculation. Instead, we can roughly say that the PL is dominated by excitonic interactions up to the electron density at which the renormalization energy is comparable with the exciton binding energy. Approximately at this density, excitons become unstable, or in other words the excitonic interaction is significantly screened by free electrons, and at higher densities, the recombination of practically unbound electrons and holes mainly appears. The same effect has been observed by Kappei *et al.*[17] They reported PL measurements on a QW with a wide range of electron-hole pair densities (from excitonic to the free carrier regime) and the maximum of the PL line remained almost unchanged. In our case, the excitonic origin of the PL at $U_{pn} = 0.0 - 0.3$ V was proven also by the quadratic shift of the PL energy with $B_\perp$ as will be shown later. The mutual electron-hole Coulomb interaction plays an important role in the optical recombination also at higher electron densities, when particles are not bound to a stable exciton. This occurs for electrons close to the Fermi level, in particular. We will deal with this problem later.

Another important feature not closely discussed up to now is the behavior of holes in our DQW. In general, a relatively broad PL spectrum is usually observed in a high density electron-hole plasma[18] or at low hole densities, when holes are localized in a disordered potential. The spread of hole wave function in the reciprocal space then allows the recombination of electrons from the bottom of the subband, as well as from the Fermi level. Figures 3(a) and 3(b) summarize the spectra gained under excitation intensities I_0, $0.1I_0$, and $0.05I_0$ at the particular bias and magnetic field. These figures illustrate that the shape of PL spectra gained at the bias close to the flat-band regime ($U_{pn} \cong +1.8$ V) or lower is almost insensitive to the excitation intensity in the chosen interval. Hence, we can conclude that the hole localization should be responsible for a relatively broad PL spectrum (up to 8 meV). We suppose that holes have a small localization energy and are strongly scattered by large inhomogeneities and potential fluctuations. This type of hole localization, enabling electron recombination in a wide interval of momentum, was identified by Tarasov *et al.*[19] Therefore, the localization energy was neglected in our calculation and hole energy was taken at the bottom of the hole subband B. For the sake of completeness, the spectra insensitive to the excitation intensity could be obtained also when the low density hole gas is Boltzmann distributed, but this possibility would lead to peaks in the PL spectra much narrower than observed.

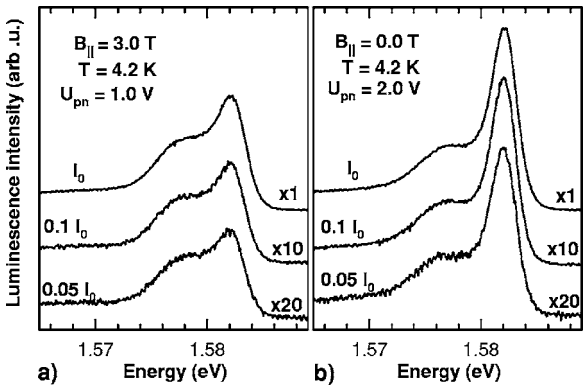

FIG. 3. The PL spectra at excitation intensities I_0, $0.1I_0$ and $0.05I_0$ for (a) $U_{pn} = +1.0$ V, $B_\parallel = 3.0$ T and (b) $U_{pn} = +2.0$ V, $B = 0.0$ T. The PL intensities are multiplied by the factor 10 and 20 for excitation intensity $0.1I_0$ and $0.05I_0$, respectively.

Independently, also another assertion can be done on the basis of Fig. 3. The optical excitation in the chosen interval of intensities does not practically affect the electron density. Hence, the photogenerated electrons with energies above the quasi-Fermi level in DQW, which is fixed by the applied bias U_{pn}, are drained from 2DEG into the electric contact. The photogenerated electrons arise not only in DQW but also in the undoped ternary regions near the DQW. Note that the absorption of photons with energy below the band gap of $Ga_{0.7}Al_{0.3}As$ is allowed by the Franz-Keldysh effect, as indicated by the observed photocurrent that was in the range of $\lesssim 100$ nA at $U_{pn} = 0.0$ V and intensity I_0.

B. PL in perpendicular magnetic field

The PL experiment in perpendicular field $B_\perp$ was performed in order to obtain a deeper insight into the electron subband structure due to the expected quantization of a 2DEG into Landau levels (LLs). The PL spectra at the constant bias $U_{pn} = +1.0$ V as a function of $B_\perp$ are shown in Fig. 4. The LLs are observable in the PL spectra as soon as the magnetic field achieves the value of $B_\perp = 3.0$ T and in the

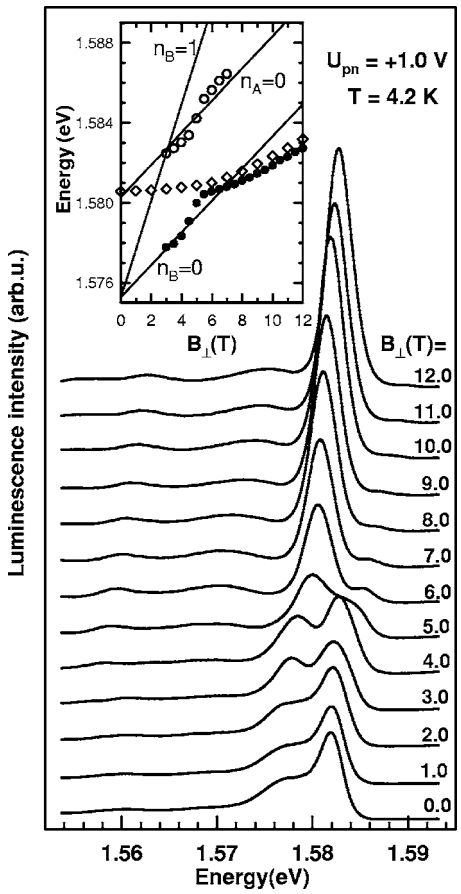

FIG. 4. Evolution of PL spectra with the magnetic field $B_\perp$ perpendicular to the layer at the bias $U_{pn}=+1.0$ V. The inset contains the fan diagram, where the full circles (●) correspond to the LL $n_B=0$ and open circles (○) to LL $n_A=0$. The full lines show calculated energies of LLs $n_{A,B}=0$ and $n_B=1$ for electron mass $m_e=0.072m_0$. Diamonds (◇) show the diamagnetic shift of the magnetoexciton line with $B_\perp$ observed at $U_{pn}=0.0$ V.

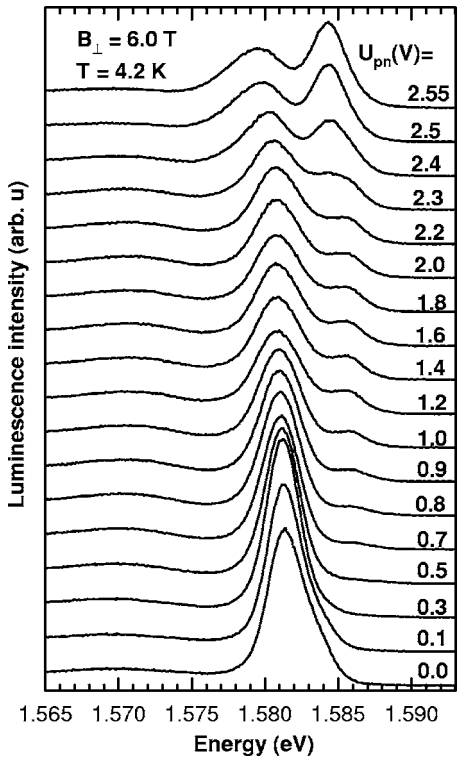

FIG. 5. Bias dependence of PL spectrum at $B_\perp=6.0$ T.

interval $B=3.0-4.5$ T, two local maxima are clearly observed. The maximum with a lower energy corresponds to the recombination from the zero LL of the bonding subband ($n_B=0$) and the maximum at the higher energy originates from the recombination of electrons from LL $n_A=0$. The peaks related to excited LLs $n_{A,B}\geqslant 1$ were not directly resolved in our PL spectra. We explain this by the fact that above $B_\perp=3.0$ T, when the splitting into LLs becomes distinguishable, all excited LLs including the lowest lying one $n_B=1$ are significantly exhausted. Furthermore, the peak corresponding to the weakly populated LL $n_B=1$ is likely hidden in the high energy side of the LL $n_A=0$ peak. We also speculate that the effect of LL $n_B=1$ could be identified from weak irregularities observed in the $B_\perp$ dependence of LLs $n_{A,B}=0$. The steep blueshift of the PL peaks at $B_\perp=4-5$ T could correspond to the reduced renormalization connected with the complete depletion of LL $n_B=1$, but the detailed study of this feature is out of the scope of this paper.

With the increasing field $B_\perp$, the enhanced degeneracy of LLs $\zeta=eB_\perp/\pi\hbar$ leads to a gradual depopulation of LL $n_A=0$ that becomes completely depopulated above $B_\perp\approx 7.0$ T. Whereas at $B_\perp<7.0$ T the LL energies apparently follow the expected linear dependence, above $B_\perp>7.0$ T the only partially occupied LL $n_B=0$ (we neglect the spin splitting here) allows the formation of excitons, whose binding energy gradually increases with the magnetic field. The LL blueshift then becomes slower and comparable to the shift of the magnetoexciton line at the low electron density maintained by $U_{pn}=0.0$ V, see the inset of Fig. 4.

The PL spectrum at $B_\perp=6.0$ T as a function of bias U_{pn} has been plotted in Fig. 5. At this magnetic field, LLs $n_B=0$ and $n_A=0$ are occupied only and the U_{pn} dependence enables a rough estimation of the total electron density in the DQW at the given bias. Results of the spectra decomposition, i.e., energies of LLs with $n_{B,A}=0$, as well as their peak area ratio, are shown in Fig. 6. As can be inferred, the distance between LL energies declines with the increasing electron concentration. However, this effect is relatively weak and thus we can say that the splitting of B and A subbands amounts to ≈ 5 meV. The ratio of peak areas in Fig. 6 roughly corresponds to the relative occupation of LLs. The LL $n_A=0$ appears in the spectra above $U_{pn}=+0.7$ V and its intensity increases rapidly up to $U_{pn}=+1.2$ V. Above this value, the peak area ratio and thus also the total electron density rises slowly and a further strong increase follows at $U_{pn}>+2.0$ V. Let us recall that the same behavior has already been shown at zero magnetic field in Fig. 2.

As Fig. 6 shows, the electron density is well stabilized in the interval $U_{pn}\approx+1.2-2.2$ V, i.e., in the interval around the flat-band regime, which is estimated to $U_{pn}\cong+1.8$ V. At lower bias, the electron concentration in DQW can be enhanced due to photon absorption in the ternary layers near the DQW. The generated electrons accumulate in the DQW resulting in a slightly increased density compared to that in

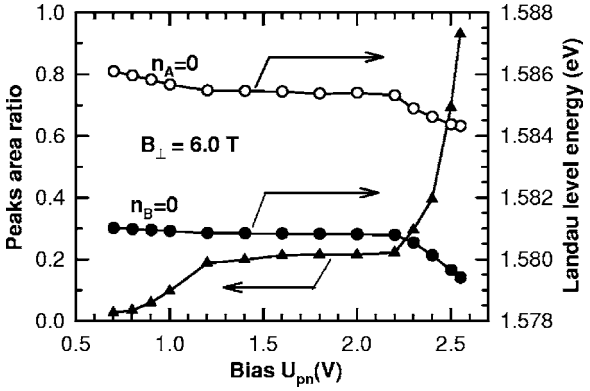

FIG. 6. The decomposition of PL spectra shown in Fig. 5. The figure summarizes the energies for $n_B=0$ (full circles, ●) and $n_A=0$ (open circles, ○) LLs at given bias U_{pn}. The ratio of the antibonding to bonding peak areas (triangles) roughly shows the relative occupation of levels. Lines serve as a guide for the eye only.

dark at the same bias. However, the total electron density in DQW is still mainly driven by the applied bias U_{pn}, as concluded above. In the flat-band position, $n^{(2)}$ should correspond to the total δ-n doping $2n_D^{(2)}$. Taking account of the relative occupation of $n_B=0$ and $n_A=0$ LLs (see Fig. 6) and the LL degeneracy at $B_\perp=6.0$ T, $\zeta=2.9\times10^{11}$ cm^{-2}, we obtain an electron density $n^{(2)}\cong3.5\times10^{11}$ cm^{-2} in the flat-band regime, i.e., only slightly above the intended value $2n_D^{(2)}$. The densities attained in this way can serve as a rough estimation only due to the neglected excitonic effects at the Fermi level. Electrons close to the Fermi level, i.e., in the partially filled LL $n_A=0$, are in the recombination process much strongly influenced by the excitonic interaction than those in the almost full LL $n_B=0$. Hence, the PL from antibonding subband could be intensified by the excitonic interaction causing thus a possible overestimation of $n^{(2)}$.

A note should be addressed to the intensity of peaks in Fig. 5. Even if the peak of LL $n_A=0$ transition at a bias $U_{pn}>+2.5$ V is higher than for the LL $n_B=0$ transition, the peak area ratio in Fig. 6 remains smaller than unity for all values of applied bias. This clearly indicates a larger peak broadening of the LL $n_B=0$ transition than that of LL $n_A=0$. We can bring out two main reasons to explain this: (i) The lower lying subband B is more affected by the potential fluctuations in the bottom of the well. (ii) Electrons in the subband A, having a node in their wave functions, are less scattered by imperfections of the very thin middle barrier in comparison with electrons in the subband B. We will include this different line broadening in our calculations later on.

The spectra in Fig. 4 were plotted in a broader spectral region to show the whole low-energy tail. With increasing $B_\perp$, a clear modulation of this tail appears. The field-induced maxima in the tail shift together with PL coming directly from DQW with increasing $B_\perp$ to higher energies. The low-energy tail, as well as its field-induced shape modulation were almost identical in the PL of all investigated structures taken from the grown wafer. Therefore, it should not be related to the defect of DQW in one particular mesa structure. However, we have to admit that the origin of the tail is not clear now. We suggest that it can be correlated with shake-up processes or with plasmon effects. The latter one is less probable because the shape of the tail is rather insensitive to the increasing electron concentration by applying higher bias voltages U_{pn}. Another explanation could be based on a PL experiment published by Tarasov *et al.*[19] Apart from the above discussed shallow localized hole states, significantly deeper lying states were also found there.

C. PL in in-plane magnetic field

In this section, the phenomena in the in-plane magnetic field $B_\parallel$ are discussed. Figure 7(a) summarizes the magnetic field dependence of the PL spectrum at a constant bias $U_{pn}=+1.8$ V, i.e., at a constant electron sheet density $n^{(2)}\cong3.5\times10^{11}$ cm^{-2}. As discussed above, the steplike shape of PL spectra at $B_\parallel=0$ T is given by the recombination of electrons from subbands B and A with heavy holes localized in the potential fluctuations, as concluded on the basis of Fig. 3. In this case, the wave functions of holes are widely spread in the reciprocal space, allowing the recombination of all electrons with a roughly equal probability. The experiment revealed a gradual damping of the PL line arising in subband A with increasing $B_\parallel$, even though the electron density $n^{(2)}$ was kept at the same level due to the constant applied bias U_{pn}. Around $B_\parallel=7.0$ T, the recombination from subband A diminishes completely and the PL from subband B takes over. A further rise of $B_\parallel$ leads to a further narrowing of the PL spectra accompanied by a moderate blueshift in its energy.

At this point, it is useful to look at Fig. 8, where PL spectra at $B_\parallel=6.0$ T are depicted as a function of U_{pn}. The spectrum develops with U_{pn} analogous to that in Figs. 2 and 5. We can observe a significant broadening of PL line above $U_{pn}=+0.5$ V, which corresponds to the creation of 2DEG and in the interval $U_{pn}=+1.2-2.0$ V, the shape of the PL spectrum remains nearly unchanged. A further increase of electron density is then observed above $U_{pn}=+2.0$ V resulting in an enhanced occupation of subband A, again in agreement with results in Figs. 2 and 5. However, the steplike shape of the PL spectrum attained at $B_\parallel=0$ T is thus not achieved even at the highest applied bias. The characteristic redshift of the PL band induced by the subband renormalization with increasing $n^{(2)}$ is also clearly seen. Hence, the dependence on U_{pn} brings analogous behavior both in the in-plane and in the perpendicular magnetic field. This observation indirectly indicates that the applied bias ensures in the in-plane magnetic field the same electron density in DQW as deduced from measurements at $B_\perp$.

D. Comparison with theory

Prior to the comparison of the experimental results with the suggested theory, a brief description of the performed calculations should be given. Our calculations are based on parameters summarized in Table I, which were taken from Davies.[20] The electron mass m_e was slightly enhanced above the bulk GaAs value due to the expected tunneling into barriers. The height of the AlAs barrier separating two QWs was adjusted to achieve a splitting of 5 meV between subbands A and B, determined experimentally at $B_\perp$. Namely, the offset[20]

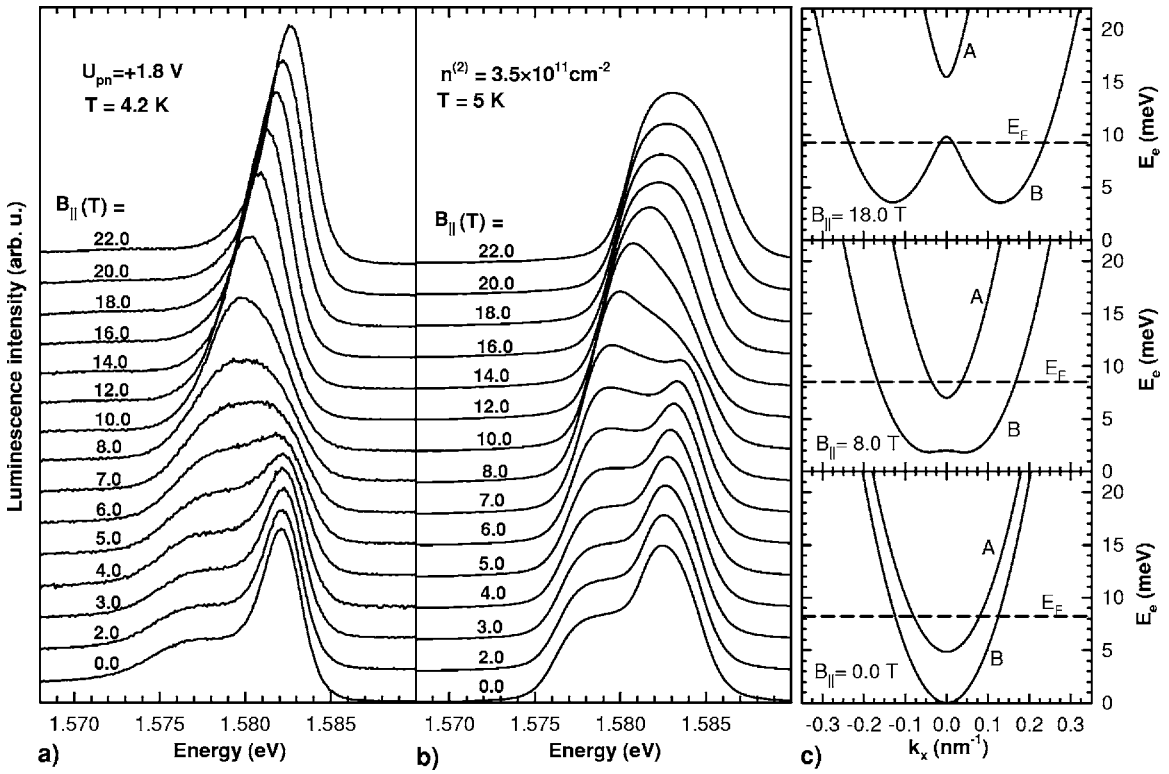

FIG. 7. (a) Normalized PL spectra in the in-plane magnetic field at the constant bias $U_{pn}=+1.8$ V. (b) Calculated PL spectra at $n^{(2)}=3.5\times10^{11}$ cm^{-2} and temperature $T=5$ K. (c) Electron dispersion in subbands B and A at $B_{\|}=0.0$, 8.0, and 18.0 T. The dashed line shows the Fermi-level energy in each case. Energies are plotted with respect to the bottom of subband B at $B_{\|}=0.0$ T.

$\Delta E_c=1120$ meV for the AlAs barrier (taken at the Γ point) was increased by an amount of 15%. We attribute that to a limited validity of the EFA method in case of a very thin, 4 ML wide, middle barrier.

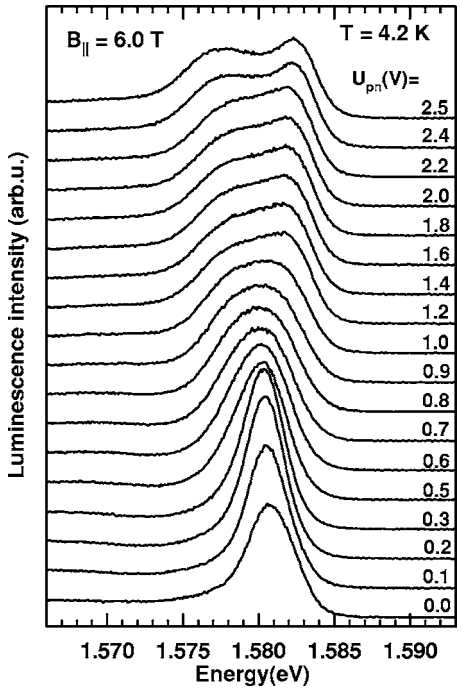

FIG. 8. PL spectra taken at $B_{\|}=6.0$ T for selected positive bias U_{pn}, i.e., at various electron densities in the DQW.

The PL spectra calculated for $n^{(2)}=3.5\times10^{11}$ cm^{-2} at a temperature of 5 K as a function of $B_{\|}$ are depicted in Fig. 7(b). These spectra were obtained using Eq. (7), where the δ function was replaced by a simple sum of the Gaussian and Lorentzian functions with the same weight in order to include both homogeneous and inhomogeneous mechanisms of PL line broadening. Another choice of the broadening function, which would prefer one of the mechanisms, would not lead to the significant changes in the results of the calculation. The lower line broadening of the PL from subband A than from subband B was used, $\sigma_B=1$ meV and $\sigma_A=0.7$ meV, as discussed above and as seen in Fig. 5. The sum in Eq. (7) runs over both occupied electron subbands ($i=1,2$) and a single energetic level E_h of localized holes. This energy of shallow localized holes was taken at the bottom of the hole subband B. Owing to the hole localization, the overlap integral in Eq. (7) is supposed to be independent of k_x and is thus not involved in the calculation.

Our calculations have also shown that 1 ML AlAs layers placed in the heterojunctions are improper to be included in our calculations using the common EFA method, because it

TABLE I. Parameters used in the calculations. The valence and conduction band offsets ΔE_v, ΔE_c, and GaAs band gap energy E_g^{GaAs} are given in meV. The value ΔE_c is valid for the molar fraction $x<0.45$ only. m_0 represents the free electron mass.

m_e	m_h	ϵ_r	ΔE_v	ΔE_c	E_g^{GaAs}
$0.072m_0$	$0.5m_0$	12.5	$474x$	$773x$	1519

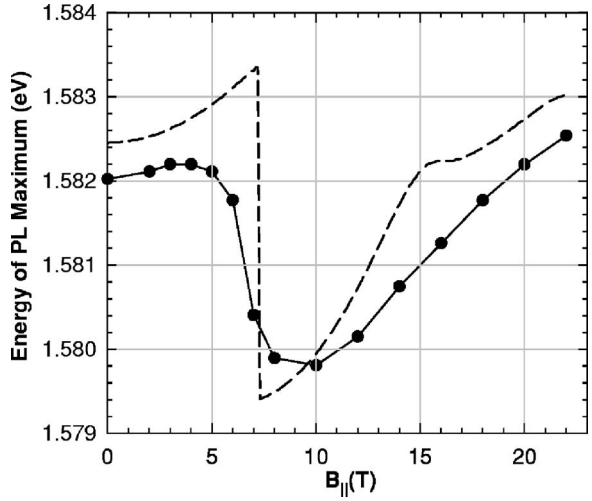

FIG. 9. The energy of the PL maximum as a function of $B_{\|}$ (closed circles) in comparison with the theoretical line (dashed line) attained for $n^{(2)}=3.5\times10^{11}$ cm^{-2}. The experiment corresponds to the measurements at $U_{pn}=+1.8$ V. The line connecting the experimental points serves as a guide for the eye only.

gives unacceptable high recombination energies in comparison with the experiment. Hence, we suppose that these layers only smooth the roughness of the heterojunctions and do not form a homogeneous AlAs monolayer. However, also in this case, these smoothing layers likely enhance the observed recombination energy. This fact together with the neglect of the hole localization energy limits the accuracy of our calculations. The calculated position of PL structure is thus given with the accuracy of several meV. We should take this into account, when the theory and experiment are compared (Figs. 2 and 7).

The calculation at $B_{\|}=0.0$ T provides an expected steplike spectrum reflecting recombination from both occupied subbands. The strength of the subband A in the PL spectra gradually declines with $B_{\|}$ in comparison with strength of subband B and slightly above $B_{\|}=7.0$ T the recombination from subband B takes over. This so-called $\mathcal{N}$-type kink effect was predicted by HL (Ref. 11) and can be more deeply understood on the basis of Fig. 7(c), where the calculated electron dispersions in the k_x direction, i.e., perpendicular to the applied in-plane magnetic field, are shown at $B_{\|}=0.0$, 8.0, and 18.0 T. The depicted position of the Fermi level E_F shows a gradual depopulation of subband A that is induced by a strong modulation of subband B dispersion. As Fig. 7(c) illustrates, two approximately parabolic-shaped minima are developed in the dispersion of the subband B at the high in-plane magnetic field. Roughly speaking, this effect doubles the total number of states close to the bottom of the subband B and induces thus the depopulation of the subband A, which is the main reason for the observation of the $\mathcal{N}$-type kink.

Another direct comparison between theory and experiment is shown in Fig. 9, where the measured and calculated $\mathcal{N}$-type kinks, i.e., position of the PL maximum as a function of $B_{\|}$, is plotted. Our simple calculation predicts a steep shift of the PL maximum from subband A to subband B at $B_{\|}=7.2$ T. This is in good agreement with the experiment, where the point of inflexion, which should correspond to the PL maxima change over from the upper to the lower subband, appears at $B_{\|}\approx6.5$ T.

The most significant feature, in which the calculation and our experiment differ, is the PL spectrum width above $B_{\|}\approx14$ T. This point must be addressed in detail. The calculated PL width above 5 meV is in contrast to the experimentally observed width $\approx3-4$ meV [cf. Figs. 7(a) and 7(b)]. To elucidate this problem, Fig. 7(c) can be consulted, where the dispersion of electrons in subband B at $B_{\|}=18.0$ T is depicted. Two minima in this dispersion curve show an effective separation of both wells in the DQW structure. Each electron in the subband B belongs to one QW only due to the Lorentzian force pushing electrons moving in the DQW plane either into the left or the right well. Hence, two parallel 2DEGs are developed and the observed PL is equivalent to the signal from two independent QWs, each with the electron density of $n^{(2)}/2$. One possible mechanism leading to the narrowing of the PL line is the electron localization in the middle of a QW, which limits the influence of imperfections in the DQW middle barrier. However, this effect itself cannot explain the whole peak narrowing because of the peak width, which is less than the calculated distance from the Fermi level to the bottom of the subband B. Therefore, we interpret the low line width as a result of the excitonic interaction, whose influence strongly increases at lower densities. Probably no stable excitons are formed, but also partially screened excitonic interaction leads to the peak narrowing.[17] In addition, the linewidth tends to increase rapidly at a higher bias (above $U_{pn}=+2.0$ V), when the electron density rises and causes probably again a transition from an excitonlike to free particlelike PL. We can also note that at high magnetic fields in the perpendicular orientation the magnetoexcitons close to the Fermi level are reported to be stable up to electron-hole plasma densities significantly higher than the electron density in our sample.[21] However, this finding cannot be easily applied to our case, when the magnetic field is oriented in the in-plane direction.

To make a short summary, our measurements were carried out on a DQW system with an electron density close to the value supposed by HL.[11] They have chosen a relatively low electron density $n^{(2)}=2.4\times10^{11}$ cm^{-2} to allow the observation of the $\mathcal{N}$-type kink effect in common DQW structures at in-plane magnetic fields of reasonable strength. PL spectra obtained from quantum well structures at densities close to $\cong10^{11}$ cm^{-2} are significantly influenced by the excitonic interaction[18] that precludes a straightforward single-particle description of the recombination process. However, our measurements have clearly demonstrated that the behavior predicted by HL can be observed. Furthermore, we are able to describe the observed effects in the quantitative way by a simple model based on the HL theory. Important deviations from their theory were registered at higher $B_{\|}$ only. Hence, the single particle model can be successfully used and even a rough quantitative description of the $\mathcal{N}$-type kink effects can be attained. At this point, we should also emphasize that with the exception of the slight adjustment of the DQW middle barrier height and of the obvious broadening factors $\sigma_{A,B}$ our calculation does not include any other free parameters.

A final note should be added for the sake of completeness. HL supposed a free hole gas instead of localized holes that

were found in our DQW structure. Therefore, our model is different in this particular way. The disordered potential as a necessary condition for a $\mathcal{N}$-type kink observation was also suggested by Kim *et al.*[15] They have identified this effect in the PL from only one particular sample that had the lowest mobility in the studied set of structures. Samples that allowed the observation of the $\mathcal{N}$-type kink are thus similar to those, where the Fermi edge singularity was studied.[19] The hole localization allows the recombination of electrons close to the Fermi level.

V. CONCLUSION

We have studied the influence of the in-plane magnetic field on the luminescence of the symmetric double quantum wells with the two-dimensional electron gas occupying two lowest subbands. A simple theoretical model similar to that suggested by Huang and Lyo[11] was applied and we have achieved a good agreement with our experimental data. Therefore, we conclude that the one-particle model can describe even in a quantitative way the luminescence of double quantum wells with the electron gas at a relatively low density under in-plane magnetic fields. Simultaneously, the effects connected with the excitonic interaction were discussed and are necessary for a more accurate description of the observed behavior.

ACKNOWLEDGMENTS

This work is a part of the research plan MSM0021620834 that is financed by the Ministry of Education of the Czech Republic. M.O. acknowledges support from the Grant Agency of Charles University under Contract No. 281/2004. The high magnetic field measurements were enabled by the program "Transnational Access to Infrastructures—Specific Support Action," Contract No. RITA-CT-2003-505474 of the European Commission.

*Electronic address: orlita@karlov.mff.cuni.cz

[1] L. V. Butov, C. W. Lai, A. L. Ivanov, A. C. Gossard, and D. S. Chemla, Nature (London) **417**, 47 (2002).
[2] L. V. Butov, A. C. Gossard, and D. S. Chemla, Nature (London) **418**, 751 (2002).
[3] S. K. Lyo, Phys. Rev. B **50**, 4965 (1994).
[4] L. Smrčka and T. Jungwirth, J. Phys.: Condens. Matter **7**, 3721 (1995).
[5] D. Simserides, J. Phys.: Condens. Matter **11**, 5131 (1999).
[6] J. A. Simmons, S. K. Lyo, N. E. Harff, and J. F. Klem, Phys. Rev. Lett. **73**, 2256 (1994).
[7] T. Jungwirth, T. S. Lay, L. Smrčka, and M. Shayegan, Phys. Rev. B **56**, 1029 (1997).
[8] O. N. Makarovskii, L. Smrčka, P. Vašek, T. Jungwirth, M. Cukr, and L. Jansen, Phys. Rev. B **62**, 10908 (2000).
[9] L. Smrčka, P. Vašek, J. Koláček, T. Jungwirth, and M. Cukr, Phys. Rev. B **51**, 18011 (1995).
[10] R. Fletcher, T. Smith, M. Tsaousidou, P. T. Coleridge, Z. R. Wasilewski, and Y. Feng, Phys. Rev. B **70**, 155333 (2004).
[11] D. Huang and S. K. Lyo, Phys. Rev. B **59**, 7600 (1999).
[12] D. M. Whittaker, T. A. Fisher, P. E. Simmonds, M. S. Skolnick, and R. S. Smith, Phys. Rev. Lett. **67**, 887 (1991).
[13] B. M. Ashkinadze, E. Linder, E. Cohen, and L. N. Pfeiffer, Phys. Rev. B **71**, 045303 (2005).
[14] Y. Kim, C. H. Perry, D. G. Rickel, J. A. Simmons, F. Klem, and E. D. Jones, in *Proceedings of the 23rd International Conference on The Physics of Semiconductors*, edited by M. Scheffler and R. Zimmermann (World Scientific, Singapore, 1996), p. 1859.
[15] Y. Kim, C. H. Perry, J. A. Simmons, and F. Klem, Appl. Phys. Lett. **77**, 388 (2000).
[16] L. Hedin and B. I. Lundqvist, J. Phys. C **4**, 2064 (1971).
[17] L. Kappei, J. Szczytko, F. Morier-Genoud, and B. Deveaud, Phys. Rev. Lett. **94**, 147403 (2005).
[18] R. Cingolani and K. Ploog, Adv. Phys. **40**, 535 (1991).
[19] G. G. Tarasov, U. Muller, Y. I. Mazur, H. Kissel, Z. Y. Zhuchenko, C. Walther, and W. T. Masselink, Phys. Rev. B **58**, 4733 (1998).
[20] J. H. Davies, *The Physics of Low-dimensional Semiconductors: An Introduction* (Cambridge University Press, Cambridge, 1997), p. 412.
[21] M. Bayer, A. Dremin, F. Faller, A. Forchel, V. D. Kulakovskii, B. N. Shepel, and T. Andersson, Phys. Rev. B **50**, 17085 (1994).